ChemPubSoc Europe

DOI: 10.1002/cmdc.201700287

CHEMMEDCHEM Communications

A Multifunctional Radiotheranostic Agent for Dual Targeting of Breast Cancer Cells

Filipe Vultos, Célia Fernandes, Filipa Mendes, Fernanda Marques, João D. G. Correia, Isabel Santos, and Lurdes Gano*[a]

A straightforward synthetic route for a new multifunctional 1,4,7,10-tetraazacyclododecane-1,4,7,10-tetraacetic acid (DOTA) derivative is described. To demonstrate the versatility of this pro-chelator for the preparation of radiolabeled hybrid compounds containing two different biological targeting moieties, an antitumor agent (e.g., a DNA-intercalating agent) and an estrogen receptor (ER) ligand (e.g., LXXLL-based peptide) were regiospecifically conjugated to the DOTA derivative. The bifunctional probe was radiolabeled with the auger electron emitter indium-111, and the resulting radioconjugate was demonstrated to induce DNA damage in vitro, which, along with the nuclear internalization exhibited in breast cancer cells, might enhance its therapeutic activity. This favorable in vitro performance suggests that these hybrid compounds could be attractive probes for theranostic applications.

Breast cancer (BC) is the most common diagnosed cancer in women and the second most frequent cause of cancer death among women worldwide.[1] The estrogen receptor (ER) is a nuclear receptor expressed in approximately 75% of breast cancer cases.[2] Therefore, ER is a well-established biomarker for prognosis and guiding treatment and is an important target for new imaging and therapeutic tools aiming to improve BC management.[3] In fact, the most pressing need in cancer management is to design effective and personalized treatments that minimize damage to the normal cells. One approach to accomplish this goal is theranostics, in which diagnosis and therapy are combined in the same molecular agent. Theranostics is particularly suitable to BC as the ER status profiling acquired by imaging can be used to target the treatment to the ER-positive cells, thus sparing normal tissue.[4]

Different types of ligands targeting cancer biomarkers have been derivatized with radiometal ions through bifunctional chelators for noninvasive in vitro imaging and therapeutic applications.[5] Radioconjugates consisting of two different molecular moieties in the same agent have been designed in order to combine different imaging modalities such as single photon emission computed tomography (SPECT) and near-infrared (NIR) optical imaging[6] or to associate the therapeutic effect of cytotoxic drugs with imaging ability.[7] Diverse multifunctional radioconjugates have also been prepared to enhance cellular retention and internalization[8] and to potentiate their uptake in specific subcellular localizations such as the nucleus[9] and the mitochondria.[10] The enhancement of nuclear uptake has been particularly important in the design of radioconjugates intended for auger electron therapy (AET). Auger-electron-emitting isotopes such as ^{111}In, ^{67}Ga, ^{64}Cu, ^{125}I, and ^{99m}Tc have attracted attention as alternatives to β-emitters due to their high-energy deposition along ultrashort trajectories that could allow a high degree of damage in malignant cells while sparing the surrounding healthy cells.[11] However, nuclear localization of these radionuclides is a prerequisite for inducing DNA damage. Introducing a peptidic nuclear localizing sequence (NLS)[9] or a small molecule that acts as DNA intercalator such as acridine orange (AO)[12] or doxorubicin[13] have been strategies applied in AET agents for achieving close proximity of the radionuclide to the DNA.

1,4,7,10-Tetraazacyclododecane-1,4,7,10-tetraacetic acid (DOTA) is one of the most widely used bifunctional chelators as it forms complexes with high thermodynamic stability and kinetic inertness with relevant radiometals used in nuclear medicine such as ^{68}Ga, ^{111}In, and ^{64}Cu.[14] Herein, we describe a synthetic orthogonal strategy toward a DOTA-based pro-chelator that can be vectorized in a regiospecific manner with two different molecular entities. A DNA intercalator (AO)[12] and an ER-targeting small peptide based on the LXXLL sequence,[15] were chosen as a proof of concept and to construct a double-vectorized agent capable of targeting the nucleus of BC cells to potentiate targeted AET. The conjugate was radiolabeled with ^{111}In, an auger electron emitter that has already been proven to have a therapeutic effect along with its well-known diagnostic value.[16]

In an effort to synthesize a macrocycle pro-chelator that could be coupled to two different biological vectors, two different pendant arms comprising orthogonally protected carboxylic acids were attached to the commercially available cyclen derivative DO2A*t*Bu. The synthetic strategy (Scheme 1) started with the monoalkylation of DO2A*t*Bu with methyl bromoacetate to give compound **I** with high yield. To prevent the formation of the bisalkylated product, the methyl bromoacetate was used in *deficit* and the addition was slow and at low temperature. In the second step, the pendant arm 5-benzyl-1-*tert*-butyl-2-bromopentanedioate,[17] was reacted with the remaining free amine of the macrocycle in a reaction that pro-

[a] *F. Vultos, Dr. C. Fernandes, Dr. F. Mendes, Dr. F. Marques, Dr. J. D. G. Correia, Dr. I. Santos, Dr. L. Gano*
Centro de Ciências e Tecnologias Nucleares, Instituto Superior Técnico, Universidade de Lisboa, Estrada Nacional 10, km 139.7, 2695-066 Bobadela LRS (Portugal)
E-mail: lgano@ctn.tecnico.ulisboa.pt

Supporting information and the ORCID identification number(s) for the author(s) of this article can be found under https://doi.org/10.1002/cmdc.201700287.

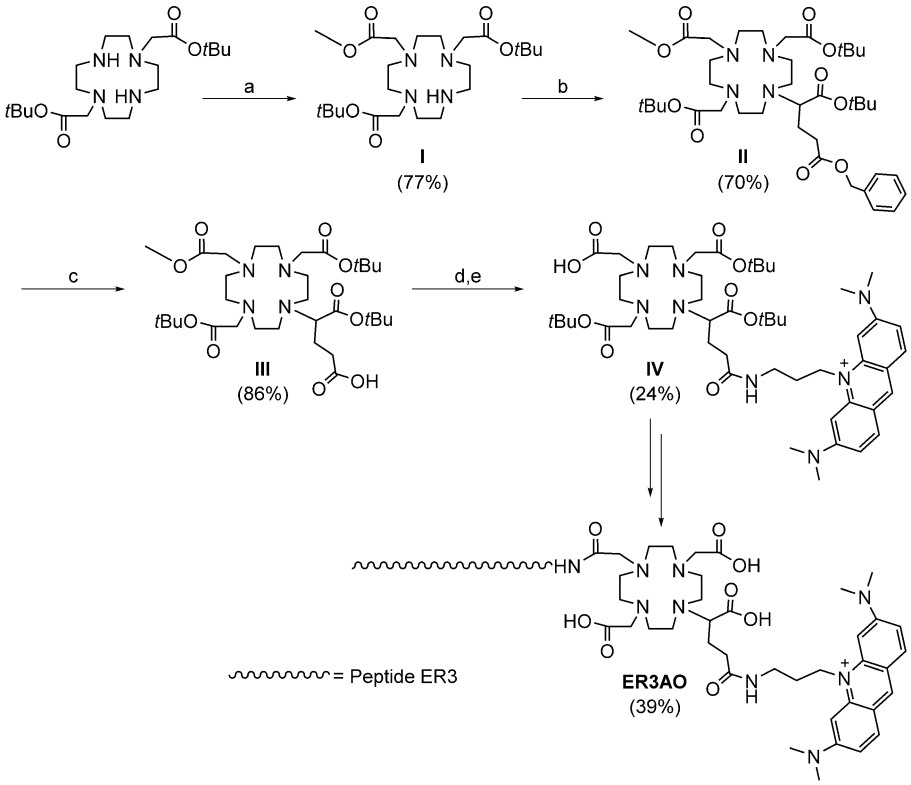

Scheme 1. Synthetic route toward the double-vectorized ligand. a) methylbromoacetate, CH_3CN, K_2CO_3, 48 h; b) 5-benzyl-1-*tert*-butyl-2-bromopentanedioate, CH_3CN, K_2CO_3, 50° C, 48 h; c) H_2 Pd/C, CH_3OH, 24 h; d) 10-(3-aminopropyl)-3,6-bis(dimethylamino)acridin-10-ium, HATU, DIPEA, DMF, 48 h; e) LiOH, THF/CH_3OH/H_2O (3:2:2), 5 h.

ceeded with high yield at 50 °C (compound **II**). The benzyl group of this pendant arm was then removed by catalytic hydrogenation[17] yielding the pro-chelator **III** with a free carboxylic acid that could be used for coupling with an amine-containing molecule. This new pro-chelator was fully characterized by ^{1}H NMR, ^{13}C NMR, and ESI-MS. After selective methyl ester deprotection of the mono-functionalized pro-chelator, this DOTA derivative could be coupled to a different biomolecule giving the possibility of obtaining a bifunctionalized macrocycle that following *tert*-butyl deprotection should yield a chelator capable of coordinating metal ions with high efficiency.

To potentiate nuclear internalization and DNA interaction of the final metal complex, an AO derivative bearing a free amine with a three-carbon spacer was selected to be conjugated to the macrocycle and was synthesized as described previously.[18] The progress of the coupling reaction was monitored by HPLC and the major peak formed was collected and analyzed by ESI-MS confirming the formation of the desired product. After 48 h, the reaction appeared to be stagnated and therefore the volatiles were removed and an extraction was performed mainly to wash the product from HATU and salts. The crude product present in the organic phase of the extraction was then used for the next step. Lithium hydroxide in a mixture of THF/CH_3OH/H_2O was used for the selective hydrolysis of the methyl ester.[19] The reaction was monitored by HPLC and after 5 h the peak corresponding to the methyl ester (starting product) completely disappeared while a peak with a slightly lower retention time, that was identified by ESI-MS as the desired demethylated compound, became the major peak in the reaction mixture. No *tert*-butyl deprotection was detected proving that this method is highly selective and efficient. The mono-functionalized pro-chelator **IV** was purified through a C_{18} Sep-Pak cartridge and characterized by NMR spectroscopy and ESI-MS. This step yielded a free carboxylic acid that could allow the coupling of a different amine-containing biomolecule thus providing the final double-vectorized macrocycle.

To prove the feasibility of this approach, a nine-mer peptide with high binding affinity toward ER was chosen as a biological vector to be coupled to the mono-functionalized pro-chelator **IV**.[15] The α-amine of the N-terminal Lysine (Lys^1) of the peptide was acetylated while the epsilon-amine of the same residue was protected with the hyper acid-sensitive group Mtt. The peptide was synthesized by solid-phase synthesis in a Sieber amide resin which allowed the simultaneous cleavage of the peptide and the Mtt deprotection in very mild acidic conditions (3% TFA in CH_2Cl_2), while keeping the other amino acid residues (including Lys^2) protected.[20] The partially protected peptide was successfully coupled in solution to the mono-functionalized pro-chelator using HATU as coupling agent. The acid-induced deprotection of the *tert*-butyl groups attached to the macrocycle ring, that occurred simultaneously with the cleavage of the side chain protecting groups of the peptide sequence, yielded compound ER3AO with three intact carboxylic acids which along with the four macrocycle nitrogen

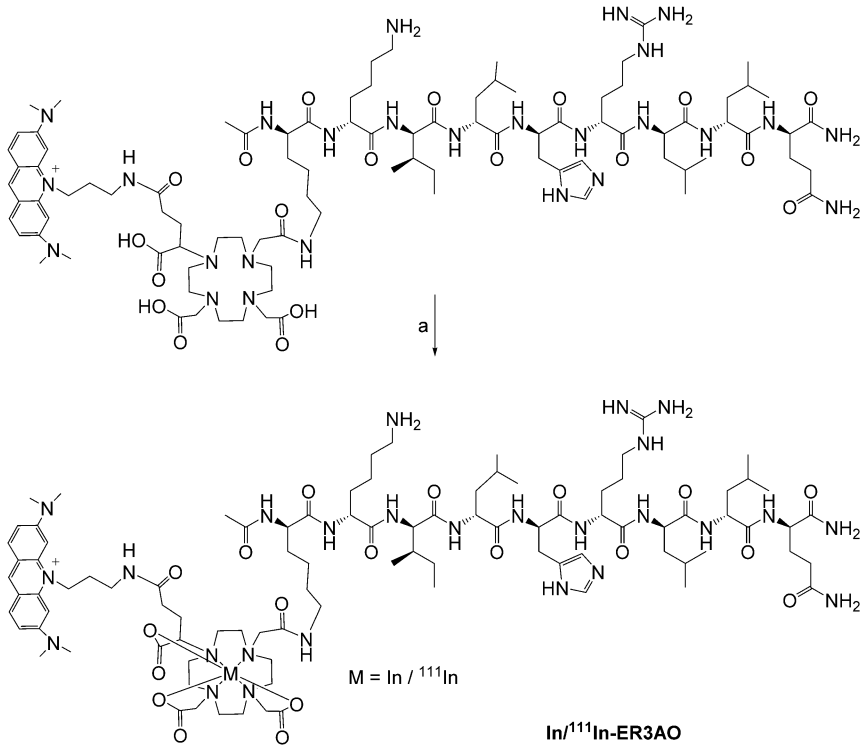

Scheme 2. Preparation of In-ER3AO/^{111}In-ER3AO. a) $InCl_3$/$^{111}InCl_3$, NaOAc (0.1 M pH 5), 95 °C, 30 min.

atoms could provide a stable and efficient chelating moiety for the complexation of indium.[21] ESI-MS spectra corroborated the identity of the final double-vectorized ligand which was further characterized by HPLC. To prove its coordinating ability, the inactive indium complex was prepared by reacting ER3AO with $InCl_3$ at high temperature (95 °C) as depicted in Scheme 2. After purification of the product, mass spectrometry supported the formation of In-ER3AO with the isotopic pattern observed in the ESI-MS spectrum being consistent with indium complexation. The double-vectorized chelator ER3AO was successfully radiolabeled with ^{111}In with high radiochemical yield and purity using standard radiolabeling conditions[22] (Scheme 2), and its chemical identity was ascertained by comparing the HPLC γ chromatogram with the HPLC UV chromatogram (Figure 1) of the inactive indium complex.

Cellular uptake of ^{111}In-ER3AO was studied in the MCF-7 BC cell line. The radioconjugate demonstrated a fast and high uptake reaching a maximum value of almost 21% after 1 h of incubation (Figure 2a). These results encouraged us to study the subcellular localization of ^{111}In-ER3AO, in particular the internalization of the radiolabeled conjugate into the cell nucleus which is a crucial feature to achieve auger-induced DNA damage by ^{111}In. The nuclear internalization study (Figure 2b) revealed a high internalization of ^{111}In-ER3AO in the nucleus with an increase over time. Remarkably, after 3 h of incubation approximately 80% of the cell-associated activity was found in the nuclear compartment of MCF-7 cells, demonstrating the efficacy of the double-vectorized probe to deliver the auger emitter ^{111}In to the nucleus of BC cells.

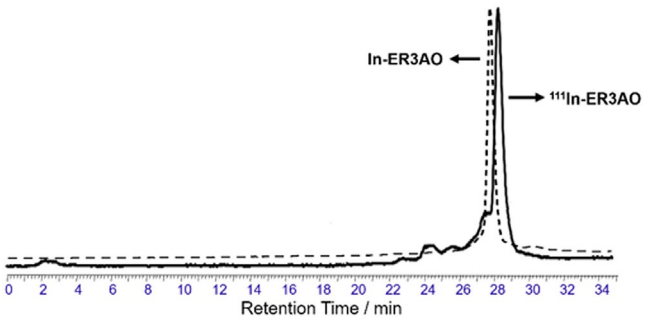

Figure 1. HPLC chromatograms of the inactive (UV detection, λ 254 nm) and radioactive (γ detection) indium complexes of ER3AO.

The ability of the ^{111}In radiolabeled probe to induce DNA damage in vitro was then tested. Various activities (MBq) of ^{111}In-ER3AO were incubated with double-stranded plasmid DNA for the time corresponding to approximately two times the ^{111}In radioactive half-life (140 h; Figures 3 and 4). Under gel electrophoresis the increase of the open-circular (OC) and linear (L) DNA isoforms were used as indicators of the auger electrons ability to induce, respectively, single strand breaks (SSB) and double strand breaks (DSB) in the parental supercoiled DNA (SC). To allow the distinction between the effects derived from the direct ionization of the DNA backbone produced by auger electrons and the indirect damaging effects caused by the radical oxygen species in the medium, DMSO was used as a radical scavenger.[23] The interaction of ^{111}In-labeled DOTA with plasmid DNA was used as comparison, as the presence of the chelator is known to prevent ^{111}In from binding to DNA.[24]

The quantification of the results of the experiments performed in the absence of DMSO (Figure 4, left columns) re-

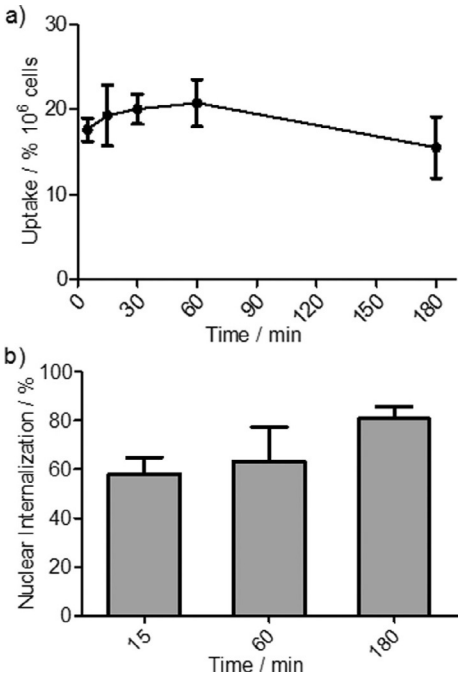

Figure 2. Cellular uptake and nuclear internalization of ^{111}In-ER3AO in MCF-7 cells. a) Activity associated with the cells (cellular uptake) expressed as a percentage (average ± SD, $n = 3$) of the total applied activity normalized per 10^6 cells. b) Nuclear internalization expressed as a percentage (average ± SD, $n = 3$) of cell-associated activity.

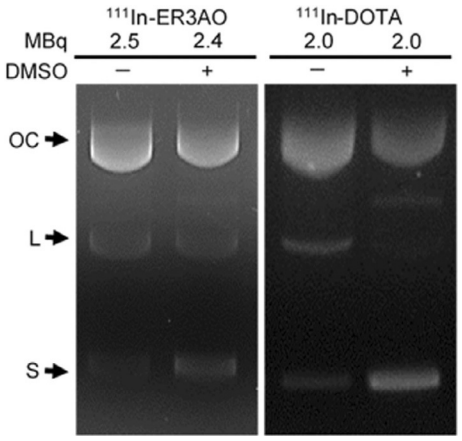

Figure 3. Representative gel of plasmid DNA incubated with ^{111}In-ER3AO and ^{111}In-DOTA (activities used are shown on the top), in the absence and in the presence of DMSO. DNA isoforms are indicated as OC: open-circular, L: linear, and SC: supercoiled.

vealed the increase of the L isoform with increasing activities for both ^{111}In-ER3AO and ^{111}In-DOTA, although this increase was more notorious for the dual-vectorized conjugate which demonstrated, for the highest activity, the formation of almost 15% of the L isoform. The inverse trend was observed with respect to the SC DNA isoform for both radioactive complexes. However, when the incubation was performed in the presence of DMSO (Figure 4, right columns), the appearance of the L isoform was practically suppressed for ^{111}In-DOTA regardless of the activity. In contrast, for the dual targeted ^{111}In-ER3AO it

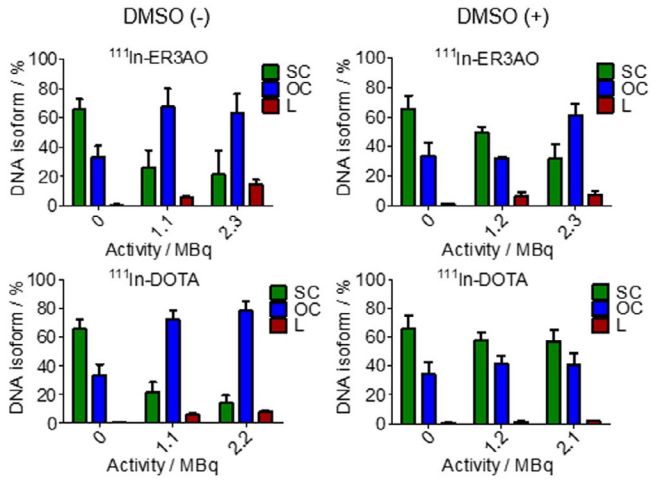

Figure 4. Quantitative analysis of the proportion (average ± SD, $n = 3$) of each DNA isoform (OC: open-circular, L: linear, SC: supercoiled) after incubation of the plasmid DNA with two different activities of ^{111}In-ER3AO and ^{111}In-DOTA, in the absence (left columns) and presence (right columns) of DMSO.

was still possible to verify an increase in both the OC (from 34 to 61%) and L (up to 7%) DNA isoforms, along with a decrease in the SC isoform with increasing activities. Therefore, ^{111}In-ER3AO was able to induce both SSB and DSB in DNA even under scavenging conditions.

These results suggest that the ^{111}In-DOTA effects in DNA are predominantly mediated by indirect mechanisms associated with the radiolysis of water, whereas ^{111}In-ER3AO causes DNA damage by a combination of both direct and indirect mechanisms. The presence of the acridine-orange-based DNA intercalating moiety in the ER3AO conjugate could explain the direct auger electrons effect as a result of the tight interaction between the coordinated radiometal and DNA, as others have previously demonstrated.[25]

In conclusion, herein we describe a straightforward and versatile synthetic approach for the double vectorization of a DOTA based pro-chelator that can allow the synthesis of multifunctional radioconjugates comprising two molecular entities (peptides and/or small molecules) with different biological targeting abilities. The concept was proved by the synthesis of a conjugate comprising an ER-targeting peptide and a DNA intercalator moiety. The ^{111}In labeled conjugate was able to localize in the nucleus of tumor cells and of inducing DNA damage in vitro, which are promising initial steps toward the development of a potential tumor theranostic agent.

Acknowledgements

F.V. thanks the Fundação para a Ciência e Tecnologia (FCT) for a PhD grant (SFRH/BD/84509/2012). This work was supported by EXCL/QEQ-MED/0233/2012 and UID/Multi/04349/2013. The QITMS instrument was acquired with support from the Programa Nacional de Reequipamento Científico (Contract REDE/1503/REM/2005-ITN) of FCT and is part of Rede Nacional de Espectrometria de Massa.

Conflict of interest

The authors declare no conflict of interest.

Keywords: cancer · indium · macrocycles · radiochemistry

[1] R. L. Siegel, K. D. Miller, A. Jemal, *Ca-Cancer J. Clin.* **2016**, *66*, 7 – 30.
[2] E. Lim, G. Tarulli, N. Portman, T. E. Hickey, W. D. Tilley, C. Palmieri, *Endocr.-Relat. Cancer* **2016**, *23*, T227 – T241.
[3] A. R. Cervino, M. Burei, L. Mansi, L. Evangelista, *Nucl. Med. Biol.* **2013**, *40*, 581 – 591.
[4] M. F. Penet, Z. Chen, S. Kakkad, M. G. Pomper, Z. M. Bhujwalla, *Eur. J. Radiol.* **2012**, *81*, S124 – S126.
[5] M. W. Brechbiel, *Q. J. Nucl. Med. Mol. Imaging* **2008**, *52*, 166 – 173.
[6] M. Morais, M. P. Campello, C. Xavier, J. Heemskerk, J. D. Correia, T. Lahoutte, V. Caveliers, S. Hernot, I. Santos, *Bioconjugate Chem.* **2014**, *25*, 1963 – 1970.
[7] S. M. Okarvi, I. Al Jammaz, *Nucl. Med. Biol.* **2010**, *37*, 277 – 288.
[8] C. A. Fischer, S. Vomstein, T. L. Mindt, *Pharmaceuticals* **2014**, *7*, 662 – 675.
[9] M. Ginj, K. Hinni, S. Tschumi, S. Schulz, H. R. Maecke, *J. Nucl. Med.* **2005**, *46*, 2097 – 2103.
[10] C. A. Kluba, A. Bauman, I. E. Valverde, S. Vomstein, T. L. Mindt, *Org. Biomol. Chem.* **2012**, *10*, 7594 – 7602.
[11] a) L. Bodei, A. I. Kassis, S. J. Adelstein, G. Mariani, *Cancer Biother. Radiopharm.* **2003**, *18*, 861 – 877; b) B. Cornelissen, K. A. Vallis, *Curr Drug Discov Technol* **2010**, *7*, 263 – 279; c) F. Buchegger, F. Perillo-Adamer, Y. M. Dupertuis, A. B. Delaloye, *Eur. J. Nucl. Med. Mol. Imaging* **2006**, *33*, 1352 – 1363.
[12] T. Esteves, F. Marques, A. Paulo, J. Rino, P. Nanda, C. J. Smith, I. Santos, *J. Biol. Inorg. Chem.* **2011**, *16*, 1141 – 1153.
[13] S. Imstepf, V. Pierroz, P. Raposinho, M. Bauwens, M. Felber, T. Fox, A. B. Shapiro, R. Freudenberg, C. Fernandes, S. Gama, G. Gasser, F. Motthagy, I. R. Santos, R. Alberto, *Bioconjugate Chem.* **2015**, *26*, 2397 – 2407.
[14] a) L. Lattuada, A. Barge, G. Cravotto, G. B. Giovenzana, L. Tei, *Chem. Soc. Rev.* **2011**, *40*, 3019 – 3049; b) C. Wängler, M. Schäfer, R. Schirrmacher, P. Bartenstein, B. Wängler, *Bioorg. Med. Chem.* **2011**, *19*, 3864 – 3874.
[15] A. M. Leduc, J. O. Trent, J. L. Wittliff, K. S. Bramlett, S. L. Briggs, N. Y. Chirgadze, Y. Wang, T. P. Burris, A. F. Spatola, *Proc. Natl. Acad. Sci. USA* **2003**, *100*, 11273 – 11278.
[16] A. Capello, E. P. Krenning, W. A. Breeman, B. F. Bernard, M. de Jong, *J. Nucl. Med.* **2003**, *44*, 98 – 104.
[17] K. P. Eisenwiener, P. Powell, H. R. Mäcke, *Bioorg. Med. Chem. Lett.* **2000**, *10*, 2133 – 2135.
[18] S. Gama, F. Mendes, T. Esteves, F. Marques, A. Matos, J. Rino, J. Coimbra, M. Ravera, E. Gabano, I. Santos, A. Paulo, *ChemBioChem* **2012**, *13*, 2352 – 2362.
[19] A. Mishra, J. Pfeuffer, R. Mishra, J. Engelmann, A. K. Mishra, K. Ugurbil, N. K. Logothetis, *Bioconjugate Chem.* **2006**, *17*, 773 – 780.
[20] M. Morais, P. D. Raposinho, M. C. Oliveira, J. D. Correia, I. Santos, *J. Biol. Inorg. Chem.* **2012**, *17*, 491 – 505.
[21] S. Liu, *Chem. Soc. Rev.* **2004**, *33*, 445 – 461.
[22] C. Decristoforo, I. H. Gonzalez, J. Carlsen, M. Rupprich, M. Huisman, I. Virgolini, H. J. Wester, R. Haubner, *Eur. J. Nucl. Med. Mol. Imaging* **2008**, *35*, 1507 – 1515.
[23] a) F. Reissig, C. Mamat, J. Steinbach, H. J. Pietzsch, R. Freudenberg, C. Navarro-Retamal, J. Caballero, J. Kotzerke, G. Wunderlich, *PLoS One* **2016**, *11*, e0161973; b) P. Balagurumoorthy, K. Chen, S. J. Adelstein, A. I. Kassis, *Radiat. Res.* **2008**, *170*, 70 – 82; c) Y. He, I. G. Panyutin, A. Karavanov, V. V. Demidov, R. D. Neumann, *Eur. J. Nucl. Med. Mol. Imaging* **2004**, *31*, 837 – 845; d) S. J. Adelstein, A. I. Kassis, *Acta Oncol.* **1996**, *35*, 797 – 801.
[24] S. K. Sahu, A. I. Kassis, G. M. Makrigiorgos, J. Baranowska-Kortylewicz, S. J. Adelstein, *Radiat. Res.* **1995**, *141*, 193 – 198.
[25] T. Esteves, C. Xavier, S. Gama, F. Mendes, P. D. Raposinho, F. Marques, A. Paulo, J. C. Pessoa, J. Rino, G. Viola, I. Santos, *Org. Biomol. Chem.* **2010**, *8*, 4104 – 4116.

Manuscript received: May 8, 2017
Revised manuscript received manuscript received: June 16, 2017
Accepted manuscript online: June 19, 2017
Version of record online: June 30, 2017